



Original article

# *In silico* Targeting, inhibition and analysis of polyketide synthase enzyme in *Aspergillus* spp

Mai M. Labib<sup>a,\*</sup>, M.K. Amin<sup>b</sup>, A.M. Alzohairy<sup>b</sup>, M.M.A. Elasztokhy<sup>b</sup>, O. Samir<sup>c</sup>, I. Saleh<sup>g</sup>, I.A. Arif<sup>g</sup>, G.H. Osman<sup>d,e,f</sup>, S.E. Hassanein<sup>a,c,\*</sup><sup>a</sup> Agriculture Genetic Engineering Research Institute (AGERI), Egypt<sup>b</sup> Faculty of Agriculture, Zagazig University, Department of Genetics<sup>c</sup> Misr University for Science and Technology (MUST), October 6, Al Jizah, Egypt<sup>d</sup> Department of Biology, Faculty of Applied Sciences, Umm Al-Qura University, Makkah, Saudi Arabia<sup>e</sup> Research Laboratories Center, Faculty of Applied Science, Umm Al-Qura University, Mecca, Saudi Arabia<sup>f</sup> Microbial Genetics Department, Agricultural Genetic Engineering Research Institute (AGERI), ARC, 12619, Giza, Egypt<sup>g</sup> Botany and Microbiology Department, Faculty of Sciences, King Saud University, Saudi Arabia

## ARTICLE INFO

## Article history:

Received 30 August 2020

Revised 28 September 2020

Accepted 7 October 2020

Available online 27 October 2020

## Keywords:

Aflatoxin  
PKS enzyme  
Aflatoxin B1  
PT domain  
Docking

## ABSTRACT

Aflatoxins are toxic and carcinogenic components produced by some *Aspergillus* species such as *Aspergillus flavus*. Polyketide synthases enzyme (PKS) plays a central role in aflatoxin biosynthesis of *Aspergillus flavus*, especially the product template (PT) domain, which controls the aldol cyclization of the polyketide forerunner during the biosynthesis of the aflatoxin pathway process. Here, we apply the *in silico* approaches to validate 623 natural components obtained from the South African Natural Compound Database (SANCDDB), to distinguish the PT domain's prospected inhibitors. From the 623 compounds, docking results showed that there are 330 different compounds with energy binding lower than the natural substrate (palmitic acid or PLM) of the Product Template domain (PT). Three factors were selected to determine the best 10 inhibiting components; 1) energy binding, 2) the strengthened chemical interactions, 3) the drug-likeness. The top ten inhibiting components are kraussianone 6, kraussianone 1, neodiospyrin, clonamine D, bromotopsentin, isodiospyrin, spongotone A, kraussianone 3, 14β-Hydroxy bufa-3,5,20,22-tetraenolide and kraussianone 7. The chemical interactions between 3HRQ domain and the natural substrate in the active site amino acids are highly similar to the 3HRQ with the top ten components, but the main differences are in the binding energy which is the best in the top ten ligands. Those ten components give successful inhibition with PT domain which will lead to the formula to be used for inhibition and control aflatoxin contamination of agriculture crop yields and lessen the degree of harming and sicknesses that are coming about because of acquiring measures of aflatoxin.

© 2020 Published by Elsevier B.V. on behalf of King Saud University. This is an open access article under the CC BY-NC-ND license (<http://creativecommons.org/licenses/by-nc-nd/4.0/>).

\* Corresponding authors at: Agriculture Genetic Engineering Research Institute (AGERI), Egypt (S. Hassanein).

E-mail addresses: [mailabibe@yahoo.com](mailto:mailabibe@yahoo.com), [mailabib@ageri.sci.eg](mailto:mailabib@ageri.sci.eg) (M.M. Labib), [osammour@hotmail.com](mailto:osammour@hotmail.com) (M.K. Amin), [alzohairy@yahoo.com](mailto:alzohairy@yahoo.com) (A.M. Alzohairy), [mohamed\\_mam82@yahoo.com](mailto:mohamed_mam82@yahoo.com) (M.M.A. Elasztokhy), [omar.samir@must.edu.eg](mailto:omar.samir@must.edu.eg) (O. Samir), [isaleh@ksu.edu.sa](mailto:isaleh@ksu.edu.sa) (I. Saleh), [iaarif@hotmail.com](mailto:iaarif@hotmail.com) (I.A. Arif), [geosman@uqu.edu.sa](mailto:geosman@uqu.edu.sa) (G.H. Osman), [sameh@ageri.sci.eg](mailto:sameh@ageri.sci.eg) (S.E. Hassanein).

Peer review under responsibility of King Saud University.



## 1. Introduction

Aflatoxins are a family of toxins produced by some species of *Aspergillus* fungi, mainly *Aspergillus flavus*, *Aspergillus parasiticus*, and *Aspergillus nomius*. They contaminate many crops, such as tree nuts, wheat, maize, cottonseed, and peanuts (Williams et al., 2004). Exposure to aflatoxin causes many diseases such as vomiting, abdominal pain, nausea, convulsions acutely, hepatotoxicity, teratogenicity, hepatocellular carcinoma, and immunotoxicity, according to (Aayush and Evelyn, 2020). The DNA information of *Aspergillus* is organized in 8 chromosomes, including the 54th cluster of 30 genes that are responsible for aflatoxin production and are regulated by aflR and aflS transcription factors. Aflatoxins are considered polyketide-derivate, which demand hexanoate units to

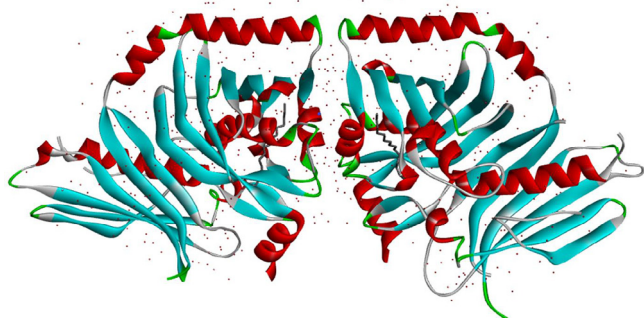


Fig. 1. The 3D structure of 3HRQ domain with its two identical chains A and B, 1.80 Å resolution, and 0.223 R-Value Free.

start biosynthesis by transforming it into norsolorinic acid (NOR). The next step is the synthesis of polyketide skeletons by aflC (pkSA) gene. The 17-kDa enzyme is expressed by hypC (hypB1) gene to catalyze norsolorinic acid anthrone (NAA) into NOR. Next, Norsolorinic acid is transformed into averantin (AVN) by the aflD-gene. The biological reactions of the 30 genes continue to produce aflatoxin in its final form of AFB1, AFB2, AFG1, and AFG2 (Isaura et al., 2020).

Polyketide synthase (PKS) is a multifunctional protein and very critical in the polyketide biosynthetic pathway. Polyketide synthase consists of six domains on a single polypeptide chain, responsible for expanding the polyketide chain to construct polyketides like aflatoxins. Also, PKS represents the aflatoxin

biosynthesis pathway's backbone in the early stages (Usha et al., 2017). There were previous strategies to inhibit aflatoxin production such as gene silencing and transgenic plants. (Jonathan and Guy, 2018) illustrated that RNAi was constructed against polyketide synthase to produce transgenic maize plants, resulting in a 93% reduction of aflatoxin production. This technique cannot be applicable in many crops such as maize and wheat because it may have a harmful effect on humans and animals and undergo many experiments. Also, (Jonathan and Guy, 2018) illustrated a different technique of spreading some *Aspergillus* strains to the soil of plants, which are capable of eliminating aflatoxin producers. However, this technique cannot conserve against postharvest contamination during grain storage. Using natural components as aflatoxin inhibitors are more secure for human rather than using pesticides or chemicals. The non-toxic natural components have been used as a thriving source for producing medicines for humans and animals (Daniel et al., 2012). In this investigation, 623 unique components were examined by *in silico* docking for the first time for their ability to inhibit the production of aflatoxin. These components had isolated from some African plant species, perennial herb, and South African marine.

## 2. Materials and methods

### 2.1. Biological data, domain sequence, and 3D structure

The information on the biological functions and interactions of *Aspergillus flavus* genes and aflatoxin pathway were obtained from the Kyoto Encyclopedia of Genes and Genomes KEGG pathway

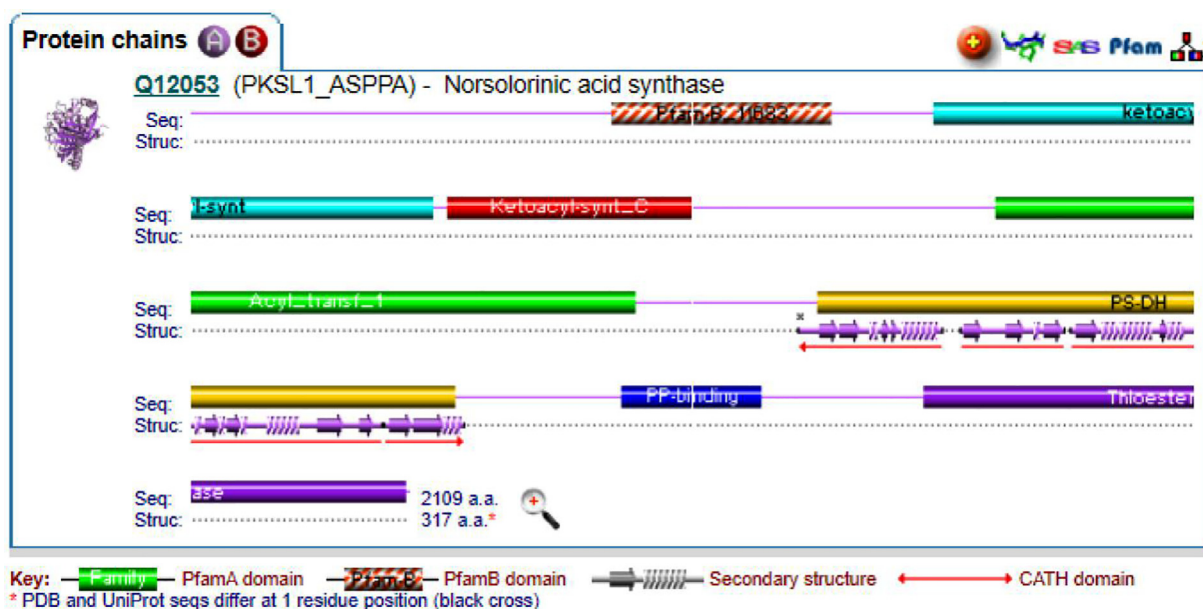


Fig. 2. The Norsolorinic acid synthase (AFLC) enzyme structure from *Aspergillus parasiticus* (strain ATCC 56,775 / NRRL 5862 / SRR143 / SU-1) showing the PfamA domain Family, the Secondary structure, and the CATH domain.

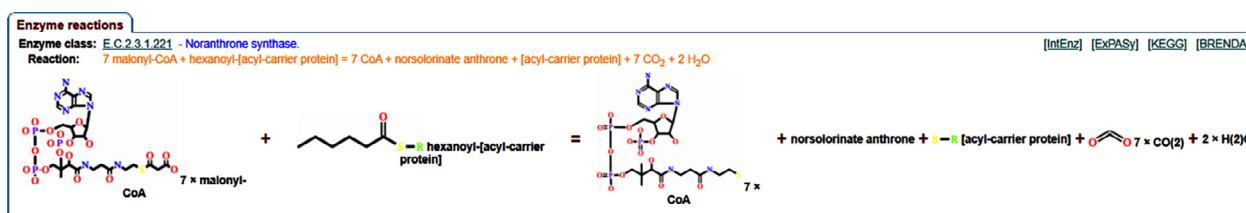
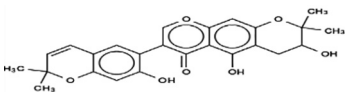
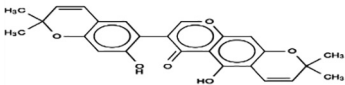
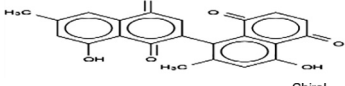
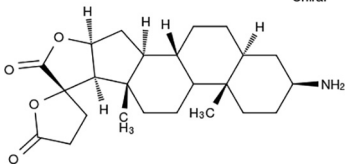
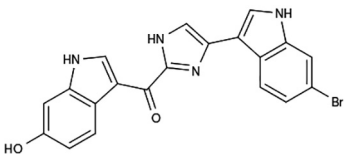
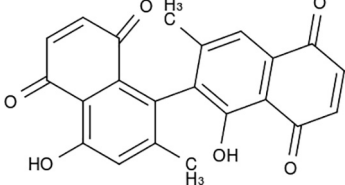
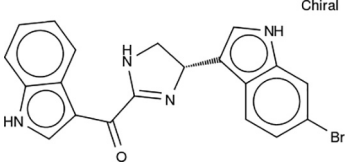
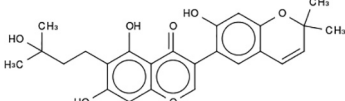
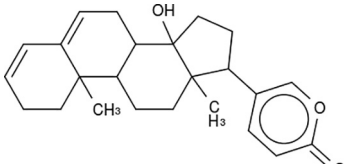
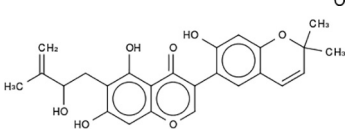


Fig. 3. 3HRQ EC Number and chemical interaction.

**Table 1**  
Ligands and their CAS Number and chemical structure.

Compound	CAS No.	Chemical structure	Source of isolation
Kraussianone 6	761456–86–4		<i>Eriosema kraussianum</i>
Kraussianone 1	497858–65–8		<i>Eriosema kraussianum</i>
Neodiospyrin	33916–25–5		<i>Euclea natalensis</i>
Clionamine D	1042138–30–6		<i>Cliona celata</i>
Bromotopsentin	112515–44–3		<i>Topsentia genetrix</i>
Isodiospyrin	20175–84–2		<i>Euclea natalensis</i>
Spongotine A	116747–40–1		<i>Topsentia pachastrelloides</i>
Kraussianone 3	497858–67–0		<i>Eriosema kraussianum</i>
14β-Hydroxybufa-3,5,20,22-tetraenolide	545–51–7		<i>Urginea epigea</i>
Kraussianone 7	761456–87–5		<i>Eriosema kraussianum</i>

database (<http://www.genome.ad.jp/kegg>). The polyketide synthase gene of *Aspergillus parasiticus* (AflC), and its functional enzyme (Norsolorinic acid synthase) (<https://www.uniprot.org/uniprot/Q12053>) was searched for Norsolorinic acid synthase structure and PT domain using the NCBI database and EMBL-EBI database (Figs. 1 and 2) (Jason et al., 2009). This enzyme belongs to polyketide synthases with EC number 2.3.1.221. As our target

PT domain, we employed the X-ray crystallographic structure derived from *Aspergillus parasiticus*, with a 1.80 Å resolution (PDB ID: 3HRQ) and a sequence with 357 amino acids (UniProtKB ID: Q12053) (<https://www.ebi.ac.uk/pdbe/entry/pdb/3HRQ>). The hexanoyl starter unit in the PT domain was provided to the acyl-carrier protein (ACP) domain by a dedicated fungal fatty acid synthase (Fig. 3).

## 2.2. Ligand preparation

About 623 natural compounds were obtained from the South African Natural Compound Database (SANCDDB). Energy minimization has been performed using Avogadro, an open-source molecular builder and visualization tool (Version 1.XX., <http://avogadro.cc/>), followed by ligand preparation using Open Babel (Version 2.3.1, <http://openbabel.org>) following the analysis pipeline described by (Patrick et al., 2019) for preparing small-molecule libraries. The Swiss ADME database (<http://www.swissadme.ch/index.php>) was used for validating the toxicity of the components. The CAS number ID and the chemical structures of the top ten selected compounds, based on their binding energies, chemical interactions, and drug-likeness are shown in Table 1.

## 2.3. Molecular docking

Initially, the protein structure was modified by removing chain B and water molecules, adding hydrogen atoms to protein and ligand, and metals were treated using the Discovery Studio software (version 2019). The structure file was saved in PDBQT format. The random setting was used for rudimentary positioning, orientation, and torsions of the ligand. Then, Auto Dock Vina (Version 2.0, <http://www.apache.org/licenses/>) was used for the grid box. Auto Grid program was utilized to generate affinity grid maps of  $48 \times 62 \times 74$  XYZ Å points and 1.00 Å spacing. After that, the polyketide synthase's active sites are identified and docked with a list of molecules. Auto Dock was exquisite to rank the van der Waals. The results included binding energy and inhibition constant, which implicate chemical interactions, hydrogen bonds, and hydrophobic regions. LIGPLOT was utilized for analyzing the

hydrophobic and H-bond interactions between the ligands and domain complexes. They were further visualized in 3D using PyMOL. Interactions complex of each ligand – 3HRQ domain were analyzed to define binding efficiency, according to (Shraddha et al., 2019).

## 3. Results and discussion

### 3.1. Drug-likeness and analogs properties of the candidate inhibitors

The early detection and filtering of all the candidates' inhibitors that have toxic effect, disadvantageous constitutional and physico-chemical characteristics that may lead to disturbed bounce on multiple protein targets and indigent properties such as distribution, absorption, metabolism, toxicity, and excretion is a master agent in remission limpness rate in the medication improvement process as it had been described by (Amit et al., 2016). The suitable properties of the identified candidate inhibitors were determined. All components were assessed and checked for toxicity and drug-likeness employing SWISS-ADME (Thommas and Özlem, 2019). As exhibited in Table 2, all the selected hits had adequate molecular weight, number of H-bond donor, number of H-bond acceptors, molar refractivity, lipophilicity, water-solubility, pharmacokinetics, drug-likeness, medicinal chemistry, and colored zone.

### 3.2. Docking score

The previous *in silico* docking studies illustrated down-regulation in the expression levels of polyketide synthase A enzyme due to the inhibition by quercetin and directly causing depression of aflatoxin production and contamination levels

**Table 2**

SWISS-ADME results: the molecular weight, number of H-bond donor, number of H-bond acceptor, Molar refractivity, Lipophilicity, Water Solubility, Pharmacokinetics, Drug-likeness, Medicinal Chemistry, and Colored Zone of each compound.

Molecule	Molecular weight g/mol	No. of H-bond donor	No. of H-bond acceptors	Molar refractivity (cm <sup>3</sup> mol <sup>-1</sup> )	Lipophilicity (Log Po/w (iLOGP))	Water Solubility	Pharmacokinetics (GI absorption)	Drug likeness	Medicinal Chemistry
Kraussianone 6	<b>436.45</b>	<b>3</b>	<b>7</b>	<b>121.05</b>	3.85	Moderately soluble	High	<b>Yes</b>	PAINS: 0 alert Brenk: 0 alert
Kraussianone 1	418.44	<b>2</b>	6	120.21	3.99	Moderately soluble	High	<b>Yes</b>	PAINS: 0 alert Brenk: 0 alert
Neodiospyrin	374.34	<b>2</b>	<b>6</b>	101.30	2.53	Moderately soluble	High	<b>Yes</b>	PAINS: 1 alert quinone_A Brenk: 0 alert
Clonamine D	401.54	<b>1</b>	<b>5</b>	109.59	2.81	Moderately soluble	High	<b>Yes</b>	PAINS: 0 alert Brenk: 1 alert: more_than_2_esters
Bromotopsentin	421.25	<b>4</b>	<b>3</b>	107.33	1.94	Moderately soluble	High	<b>Yes</b>	PAINS: 0 alert Brenk: 0 alert
Isodiospyrin	374.34	<b>2</b>	<b>6</b>	101.46	2.32	Moderately soluble	High	<b>Yes</b>	PAINS: 1 alert: quinone_A Brenk: 0 alert
Spongotine A	407.26	<b>3</b>	<b>2</b>	113.76	1.94	Moderately soluble	High	<b>Yes</b>	PAINS: 0 alert Brenk: 0 alert
Kraussianone 3	438.47	<b>4</b>	<b>7</b>	123.50	3.63	Moderately soluble	High	<b>Yes</b>	PAINS: 0 alert Brenk: 0 alert
14β-Hydroxybufa-3,5,20,22-tetraenolide	366.49	<b>1</b>	<b>3</b>	107.75	3.36	Moderately soluble	High	<b>Yes</b>	PAINS: 0 alert Brenk: 0 alert
Kraussianone 7	436.45	<b>4</b>	<b>7</b>	122.99	3.71	Moderately soluble	High	<b>Yes</b>	PAINS: 0 alert Brenk: 1 alert: isolated_alkene

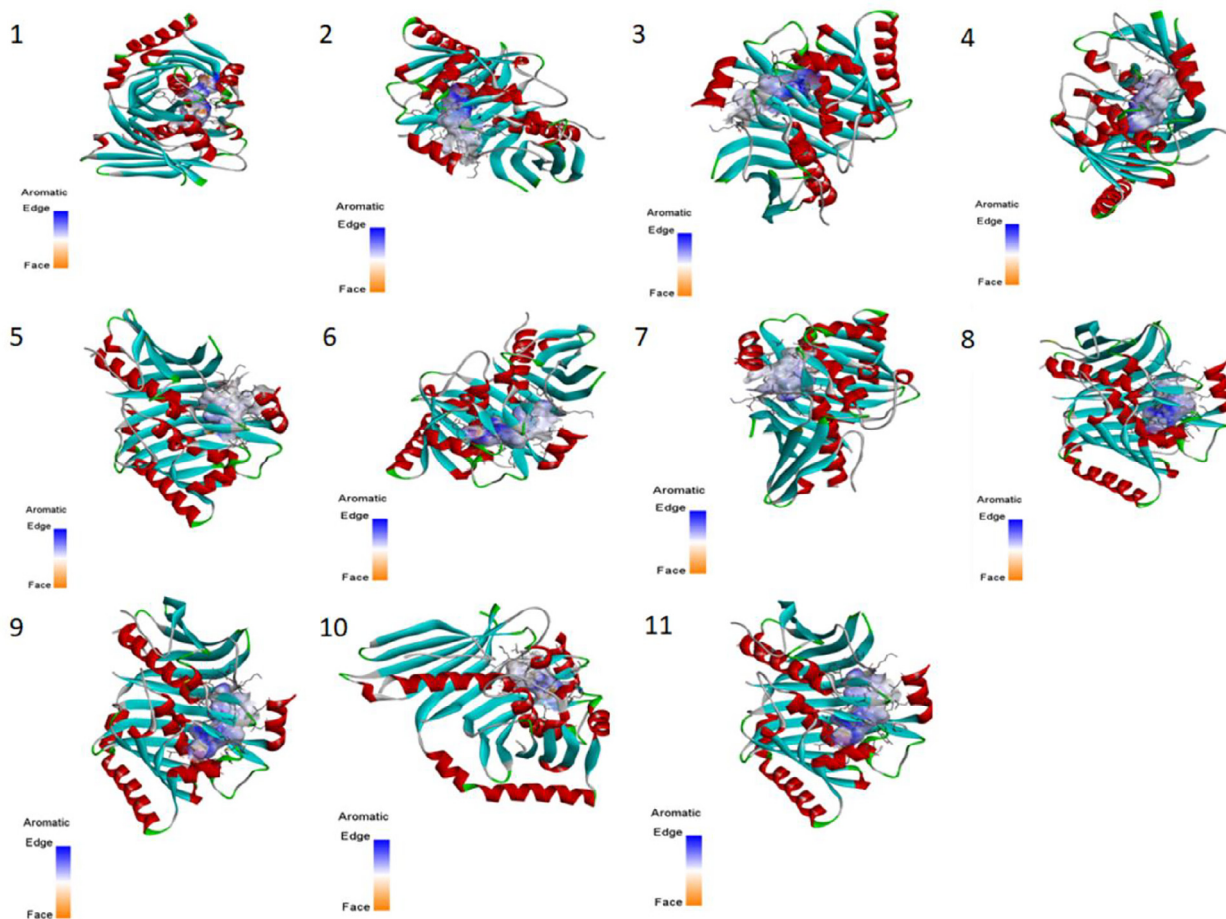


**Fig. 4.** The PKS (PT domain) - interaction with the substrate and the top ten inhibitors (Structural View). 1) The interaction with the substrate. 2) The interaction with the Kraussianone 6. 3) The interaction with the Kraussianone 1. 4) The interaction with the Neodiospyrin. 5) The interaction with the Clionamine D. 6) The interaction with the Bromotopsentin. 7) The interaction with the Isodiospyrin. 8) The interaction with the Spongotine A. 9) The interaction with the Kraussianone 3. 10) The interaction with the 14 $\beta$ -Hydroxybufa-3, 5, 20, 22-tetraenolide. 11) The interaction with the Kraussianone 7.

**Table 3**

Docking score for the top ten compounds and the number of conventional hydrogen bonds in each component.

Name	Binding energy	Number of Covalent hydrogen bond with 3HRQ domain
Kraussianone 6	-11.1	2
Kraussianone 1	-10.9	1
Neodiospyrin	-10.6	2
Clionamine D	-10.5	2
Bromotopsentin	-10.0	1
Isodiospyrin	-9.8	1
Spongotine A	-9.7	1
Kraussianone 3	-9.6	1
14 $\beta$ -Hydroxybufa-3,5,20,22-tetraenolide	-9.6	1
Kraussianone 7	-9.5	2
Substrate	-7.3	2

(Sudharsan et al., 2019). So, *in silico* drug design parameters such as docking is very useful to discover potent inhibitors for aflatoxin, especially for polyketide synthase protein. The 3HRQ domain - interaction with the natural substrate (PLM) and the 623 compounds were analyzed. The binding energy scores of the 330 compounds were identified and showed powerful interactions with the plurality of the 3HRQ domain compared with PLM. So, ligands with its structures resort to setup more contacts with the receptor residues, leading to vigorous interaction binding energy (María et al., 2015).

The Structure view of the top ten compounds was shown in Fig. 4. From the obtained docking results, the docked natural substrate binding energy result was  $-7.3$ . In contrast, the docked kraussianone 6 component result was found to have the highest docking score of  $-11.1$  and interacted with the 3HRQ domain by two conventional hydrogen bonds with ASN A: 1568 and ASP A: 1395 amino acids and other chemical interactions were Alkyl, Pi-Alkyl, Pi-Sigma and van der waals forces (Table 2). Other compounds showed different docking results ranged from  $-10.9$  to  $-9.5$ . Thus, kraussianone 6 was a remarkable component. From the list of compounds in table 3, kraussianone 6 shows high biological inhibition activity against fungal protein PKS 3HRQ domain and docking score of  $-11.1$  and two conventional hydrogen bonds. Kraussianone 6, kraussianone 1, kraussianone 3, and kraussianone 7 were naturally isolated from the perennial herb *Eriosema kraussianum*, neodiospyrin and isodiospyrin were naturally isolated from a dioecious African plant species *Euclea natalensis*, clionamine D was naturally isolated from *Cliona celata* (called the red boring sponge), bromotopsentin was naturally isolated from Mediterranean shallow-water sponges *Topsentia genetrix*, spongotine A was naturally separated from the intertidal South African marine *Topsentia pachastrelloides*, 14 $\beta$ -Hydroxybufa-3,5,20,22-tetraenolide was naturally isolated from *Urginea epigea*. Those unique components had been extracted and identified recently from South Africa and were examined for the first time by *in silico* docking against PKS enzyme and aflatoxin production.

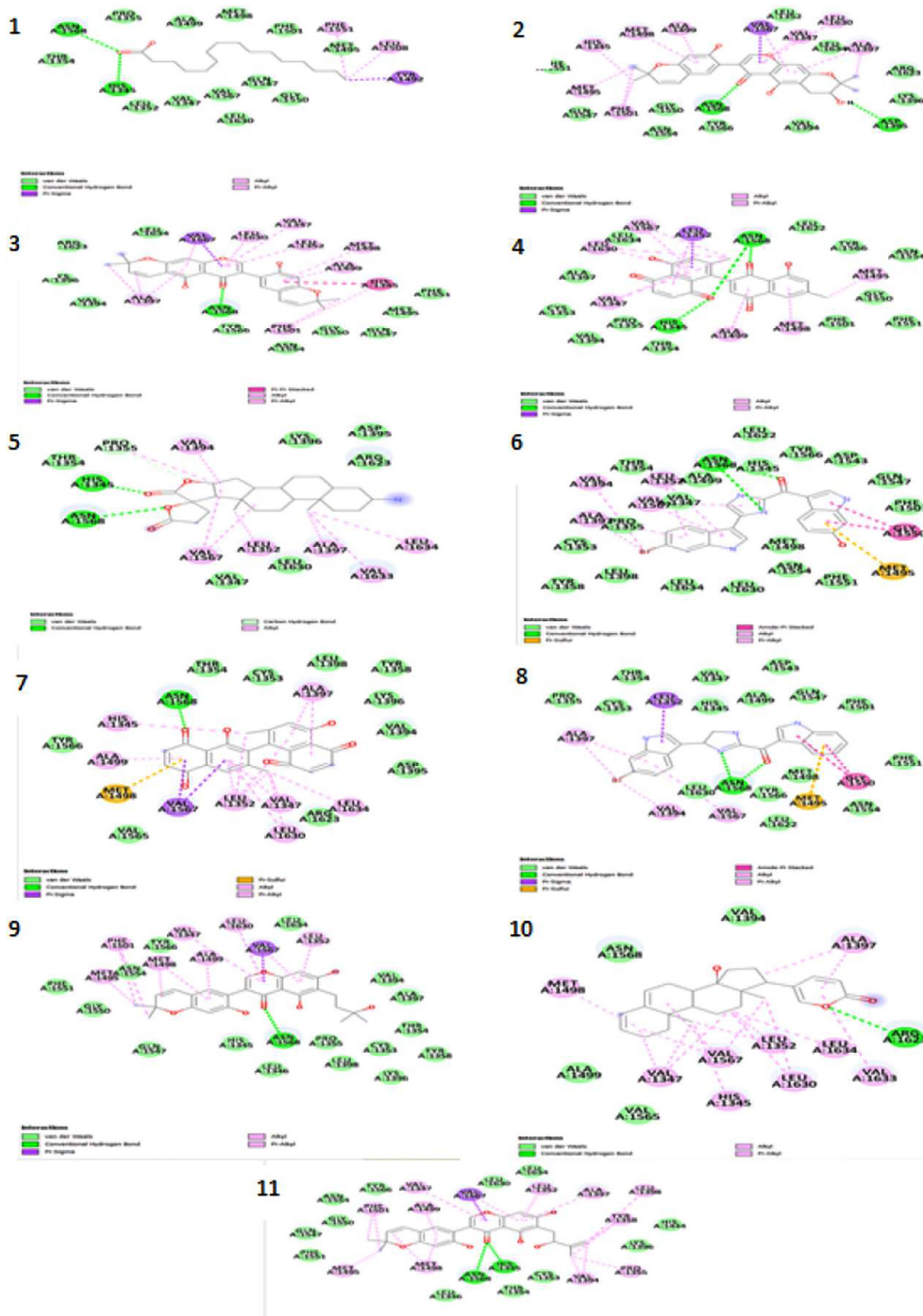


**Fig. 5.** The 2D PKS (PT domain) – chemical interaction with the substrate and the top ten inhibitors. 1) The interaction with the substrate. 2) The interaction with the Kraussianone 6. 3) The interaction with the kraussianone 1. 4) The interaction with the neodiospyrin. 5) The interaction with the clonamine D. 6) The interaction with the bromotopsentin. 7) The interaction with the isodiospyrin. 8) The interaction with the spongotine A. 9) The interaction with the kraussianone 3. 10) The interaction with the 14β-Hydroxybufa-3,5,20,22-tetraenolide. 11) The interaction with the Kraussianone 7.

### 3.3. Chemical interaction with 3HRQ domain

The computational assessment of the protein–ligand interaction of all of the ligands (natural components) with PKS' 3HRQ domain was visualized using Discovery Studio software version 2019. It shows the 2D of the chemical interaction with substrate and inhibitors such as the number of conventional hydrogen bonds which ranged from two in the substrate, kraussianone 6, neodiospyrin, clonamine D, and kraussianone 7 and one in the others inhibitors (Hong-Lian et al., 2017). Other chemical interactions such as carbon-hydrogen bond, van der waals, Pi-sigma, Pi-sulfur, Alkyl, Pi-Alkyl, Pi-pi sigma, Pi-pi stacked, and Amide-pi stacked are shown in Fig. 5. The amino acids interact with palmitic acid (ligand) ASN A: 1568 and HIS A: 1345. The secondary structure between 3HRQ and the ligands supply the best possible association of both amino acid residues. Also, the amino acid residues that associate with kraussianone 6, kraussianone 1, neodiospyrin, clonamine D, bromotoposentin, isodiospyrin, spongotine A, kraussianone 3, 14 $\beta$ -Hydroxybufa-3,5,20,22-tetraenolide, and kraussianone 7 were ASN A: 1568, HIS A: 1345, and ASP A: 1395 and those interactions were by conventional hydrogen bond which is shown in Fig. 5.

Hydrophobic regions between PKS (PT domain) and the substrate and the top ten inhibitors were different from each inhibitor to the other and ranged from the brown color, which represents the hydrophobic regions, and the blue color, which represent the hydrophilic regions (Fig. 6). The number of hydrophobic atoms is significant in hydrophobic interactions in drug resolving due to the rising of the binding consanguinity between target drug mediators. The binding consanguinity and drug effectiveness correlated with hydrophobic interactions were advanced by the association at the hydrogen bonding site. On the other hand, water molecules' subsistence in the hydrophobic locus is very important to make this region quite flexible. The augmentation in the number of hydrophobic atoms in the specific active core site of the drug-target complex will lead to an increase in the biological inhibition activity of the drug leadership (Rohan et al., 2010).

On the other hand, hydrogen bond interaction is shown in Fig. 7, which establishes more informatics of association's structural view. The results ranged from the pink color, representing the H-donor, and green color representing the H-acceptor. The significance of hydrogen bonds, a target–drug complex's binding alliance, was described previously (Rohan et al., 2010). It was clarified that

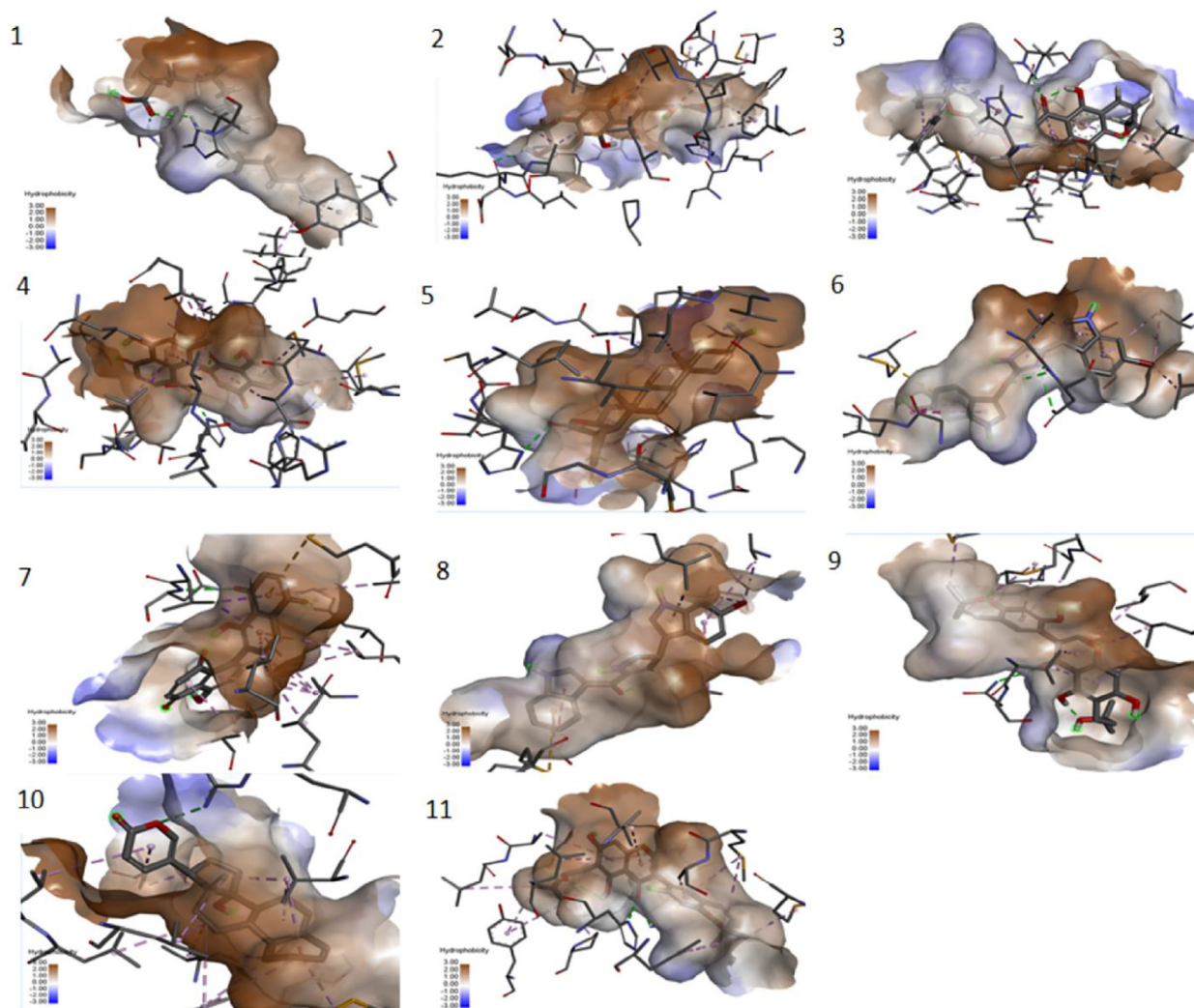


**Fig. 6.** Hydrophobic Interaction between PKS (PT domain) and the substrate and the top ten inhibitors. 1) The interaction with the substrate. 2) The interaction with the kraussianone 6. 3) The interaction with the kraussianone 1. 4) The interaction with the neodiospyrin. 5) The interaction with the clonamine D. 6) The interaction with the bromotoposentin. 7) The interaction with the isodiospyrin. 8) The interaction with the spongotine A. 9) The interaction with the kraussianone 3. 10) The interaction with the 14 $\beta$ -Hydroxybufa-3,5,20,22-tetraenolide. 11) The interaction with the kraussianone 7.

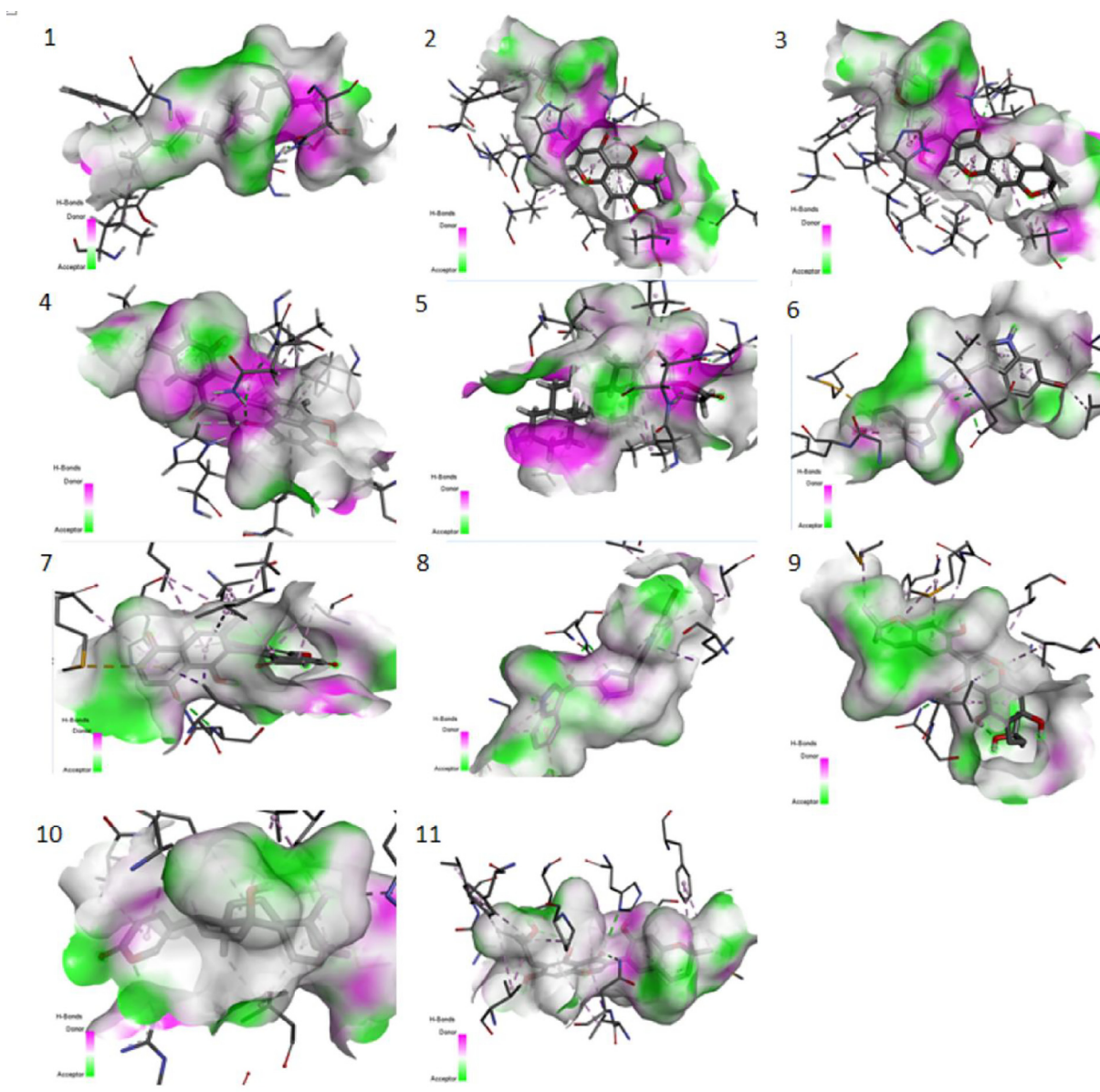


**Fig. 7.** Hydrogen bond interaction between PKS (PT domain) and the substrate and the top ten inhibitors. 1) The interaction with the substrate. 2) The interaction with the kraussianone 6. 3) The interaction with the kraussianone 1. 4) The interaction with the neodiospyrin. 5) The interaction with the clonamine D. 6) The interaction with the bromotopsentin. 7) The interaction with the isodiospyrin. 8) The interaction with the spongotine A. 9) The interaction with the kraussianone 3. 10) The interaction with the 14 $\beta$ -Hydroxybufa-3,5,20,22-tetraenolide. 11) The interaction with the kraussianone 7.

the domain-ligand complex interface increased the binding cognition of complex molecules and was upgraded for its hydrogen bonds and the hydrophobic interactions. The enzyme's standard case changes, such as hydrophobic, hydrophilic, H-donor, and H-acceptor, can lead to inactivation for this enzyme (Nicholls et al., 2000).

### 3.4. 2D interaction map

The brief 2D interaction map was generated using the LIGPLOT + program. The key residues, such as numbering according to each protein's catalytic domain protein–ligand complex and protein–substrate complex interaction analysis, stabilize the ligands inside the subsite pockets, performed on each complex were determined (Sourav et al., 2019). The shared interactions between the 3HRQ domain and substrate are highly similar to

the domain with the top ten ligands, but the main differences are binding energy, which is the best in the top ten ligands. The comparison between the substrate and kraussianone 6 in the interactions with the 3HRQ domain showed similarity in 11 interactions. Also, 11 interactions were shared with kraussianone 1, 12 interactions with neodiospyrin, 6 interactions with clonamine D, 10 interactions with bromotopsentin, 5 interactions with isodiospyrin, 10 interactions with Spongotine A, 13 interactions with Kraussianone 3, 6 interactions with 14 $\beta$ -Hydroxybufa-3,5,20,22-tetraenolide, and 14 interactions with Kraussianone 7 which is shown in in red circles Fig. 8.

### 4. Conclusions

In conclusion, about 623 natural components were examined to act as natural inhibitors for the 3HRQ domain to block the polyke-



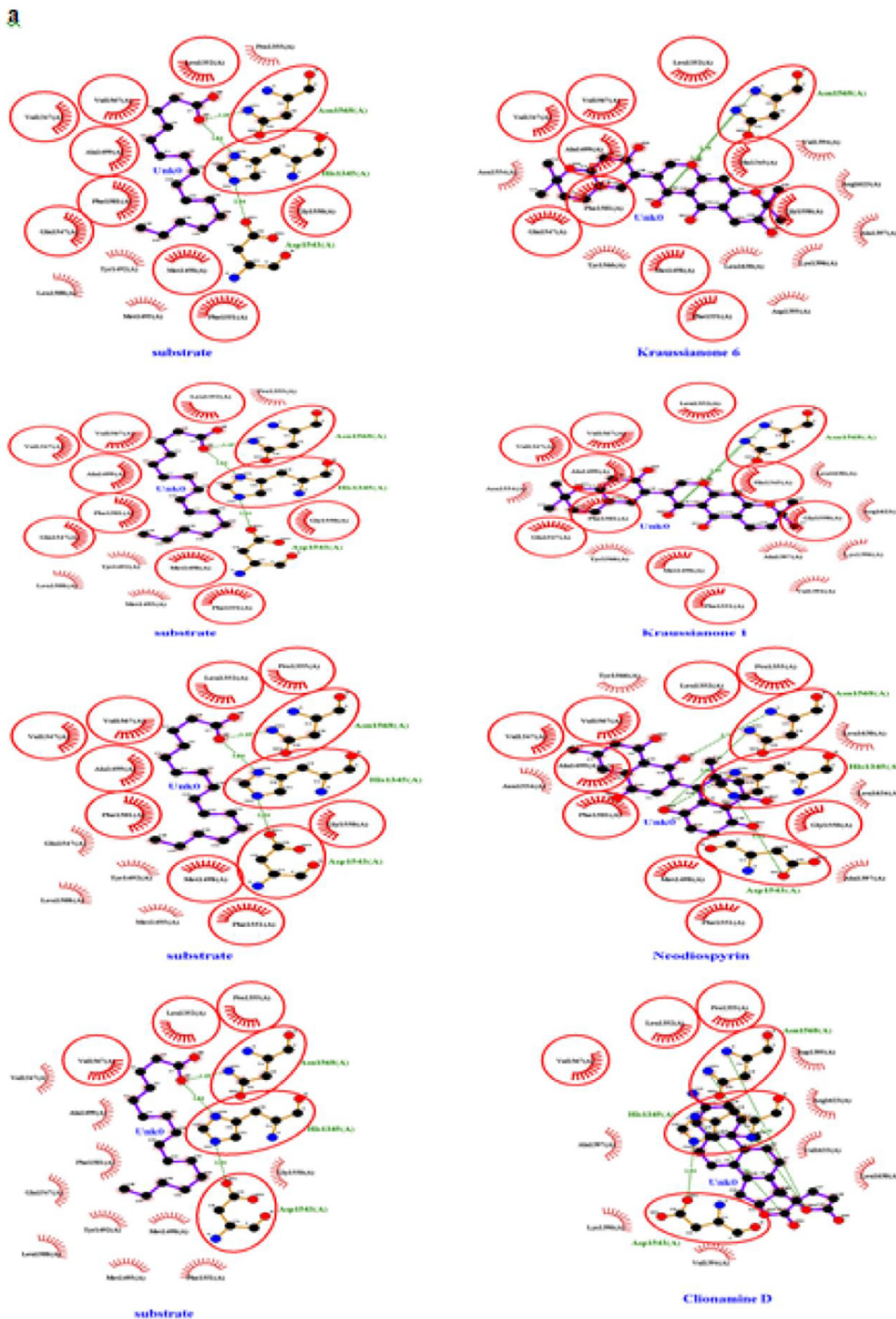


**Fig. 8.** The interactions between the active site of the 3HRQ domain of PksA with the substrate and ten different ligands, kraussianone 6, kraussianone 1, neodiospyrin, clonamine D, bromotopsentin, isidiospyrin, spongotine A, kraussianone 3, 14β-Hydroxybufo-3,5,20,22-tetraenolide, and kraussianone 7 using LigPlot.

b

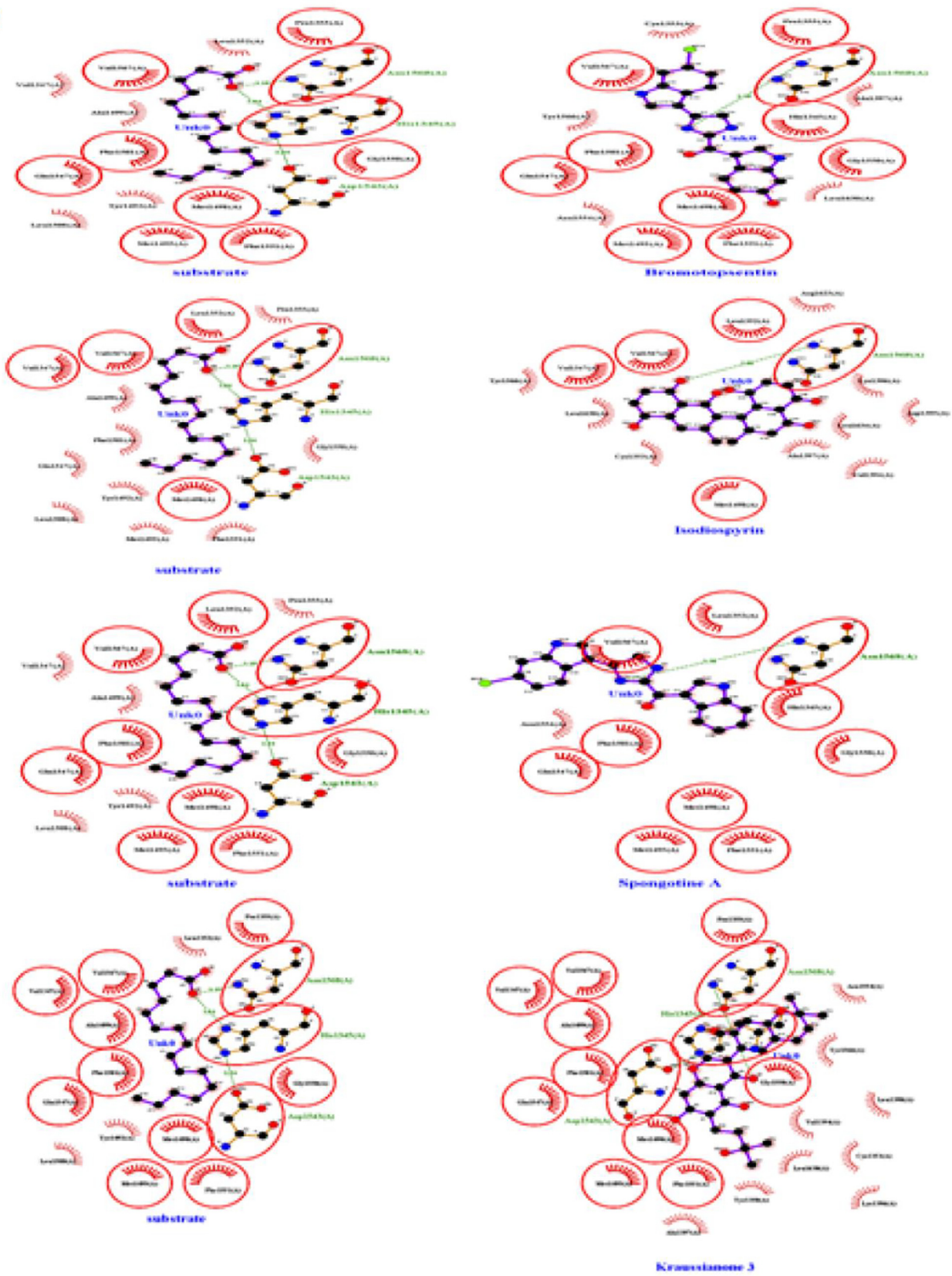


Fig. 8 (continued)

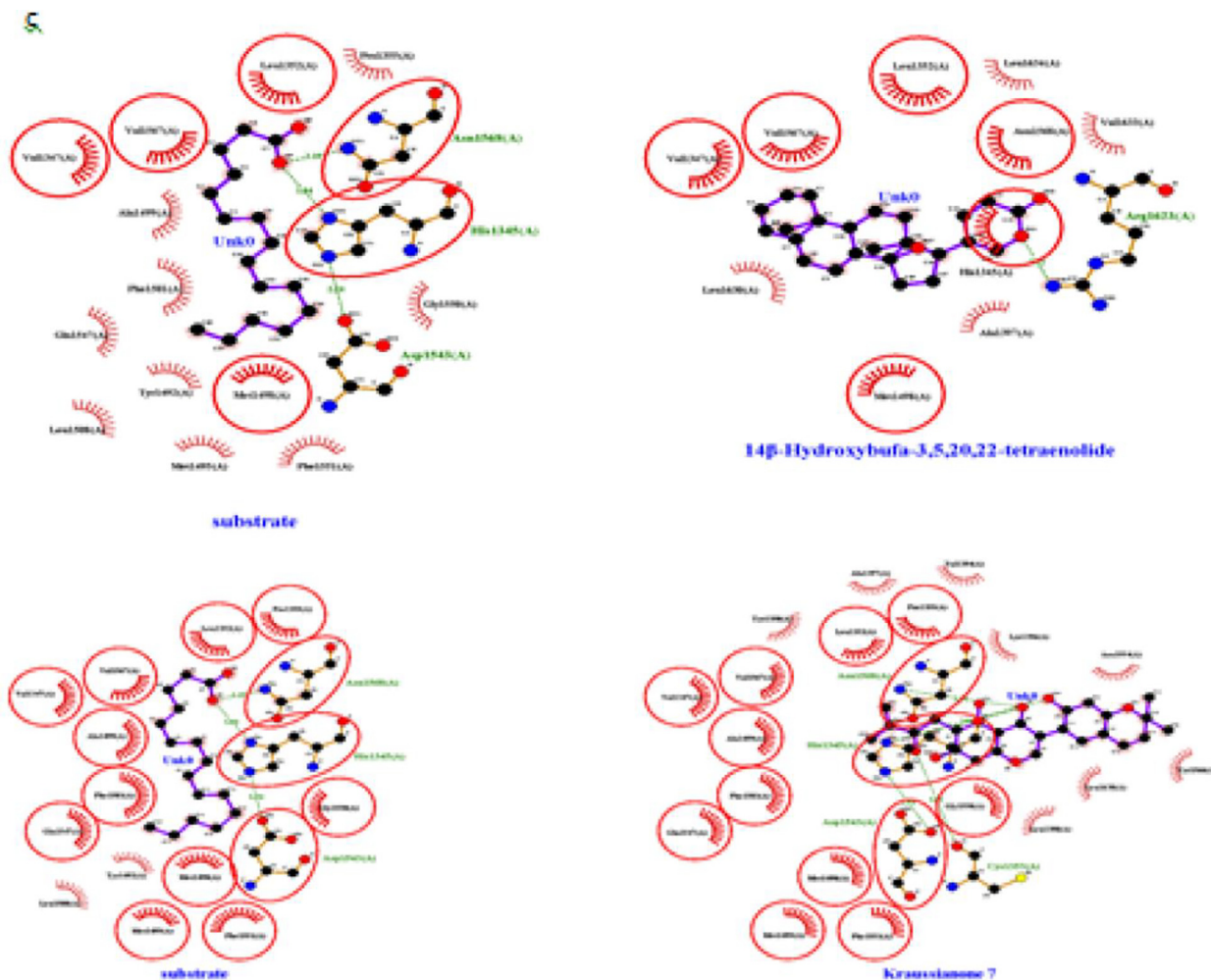


Fig. 8 (continued)

tide synthesis enzyme. Docking results showed that about 330 proved their ability to act as inhibitors. The 330 components were filtered to elicit the best ten components. The results showed kraussianone 6, kraussianone 1, neodiospyrin, clionamine D, bromotopsentin, isodiospyrin, spongotone A, kraussianone 3, 14β-Hydroxybufa-3,5,20,22-tetraenolide, and kraussianone 7 were the best depending on the lowest binding energy, the best in chemical interactions, and the best in drug-likeness. Those components would lead to the formula for inhibition and control aflatoxin contamination of agriculture crop yields and lessen the degree of harming and sicknesses.

**Declaration of Competing Interest**

The authors declare that they have no known competing financial interests or personal relationships that could have appeared to influence the work reported in this paper.

**Acknowledgments**

Research of this work was supported by the Agriculture Genetic Engineering Research Institute (AGERI), Zagazig University, and Misr University for Science and Technology (MUST) in Egypt. ML offers sincere thanks and appreciation for MA, AZ, SH, and ME for this work’s supervision. The authors would love to dedicate this

work to the deceased Prof. Gamal Osman, who contributed generously to the current research. Finally, they would also like to thank the reviewers for positive criticism to improve the quality of the manuscript.

**Ethics approval and consent to participate**

Not applicable.

**Consent for publication**

Not applicable.

**Availability of data and materials**

All relevant data are within the manuscript.

**Funding**

Not applicable.

## Authors' contributions

The authors contributed to the work done in the manuscript as follows: ML conceived of the presented ideas, ML, SH, and OS developed the theory and performed the computations and conducted the experiments, presented the data in tables and graphs. MA, AZ, SH, and ME verified the analytical methods, revised the experimental design, guided the data analyses and interpretation and manuscript revision, and supervised the findings of this work. ML prepared the preliminary version of the manuscript. GO, IA, and IS contributed to the final version of the manuscript.

## References

- Aayush, D., Evelyn, S., 2020. Aflatoxin Toxicity. StatPearls Publishing.
- Amit, P., Jeffrey, R.B., Carol, A.F., Ayyalusamy, R., 2016. Inhibition of IAPP Aggregation and Toxicity by Natural Products and Derivatives. *J. Diabetes Res.* 2016 (12).
- Daniel, A., Dias, S.U., Ute, R., 2012. A Historical Overview of Natural Products in Drug Discovery. *Metabolites* 2 (2), 303–336.
- Hong, L.L., Ying, M., Ying, M., Yu, L., Xiu, B.C., Wei, L.D., Run, L.W., 2017. The Design of Novel Inhibitors for Treating Cancer by Targeting CDC25B Through Disruption of CDC25B CDK2/Cyclin A Interaction Using Computational Approaches. *Oncotarget* 8 (20), 33225–33240.
- Isaura, C., Anthony, A., Rhoda, E., Sophie, L., Isabelle, P.O., André, E., Ali, A.T., Olivier, P., Jean, D.B., 2020. Aflatoxin Biosynthesis and Genetic Regulation: A Review. *Toxins (Basel)* 12 (3), 150.
- Jason, M.C., Tyler, P.K., Jason, W.L., Anna, L.V., Eric, A.H., Oliver, K., Shiou, C.T., Craig, A.T., 2009. Structural Basis for Biosynthetic Programming of Fungal Aromatic Polyketide Cyclization. *Nature* 461 (7267), 1139–1143.
- Jonathan, G., Guy, P., 2018. Suppressing Aflatoxin Biosynthesis Is Not A Breakthrough If Not Useful. *Pest Manag Sci.* 74, 17–21.
- María, J.G., Esteban, L., José, G., Antonio, J.N., José, F.A., 2015. Solving Molecular Docking Problems With Multi-Objective Metaheuristics. *Molecules* 20 (6), 10154–10183.
- Nicholls, P., Ignacio, F., Peter, C.L., 2000. Enzymology and Structure of Catalases. *Adv Inorg Chem* 51 (14), 10.
- Patrick, J.R., Jacob, O.S., Jennifer, L.W., Harrison, G., Guillermo, A.M., Katherine, A.M., John, J.R., Jacob, D.D., 2019. Gypsum-DL: An Open-Source Program for Preparing Small-Molecule Libraries for Structure-Based Virtual Screening. *J. Cheminform* 11 (34).
- Rohan, P., Suranjana, D., Ashley, S., Lumbani, Y., Akulapalli, S., Ashok, K.V., 2010. Optimized Hydrophobic Interactions and Hydrogen Bonding At The Target-Ligand Interface Leads The Pathways Of Drug-Designing. *PLoS ONE* 5, (8) e12029.
- Shraddha, T., Sonia, K.S., Jata, S., 2019. Docking Analysis Of Hexanoic Acid And Quercetin With Seven Domains Of Polyketide Synthase A Provided Insight into Quercetin-Mediated Aflatoxin Biosynthesis Inhibition in *Aspergillus flavus*. *Biotech* 9, 149.
- Sourav, P., Vinay, K., Biswajit, K., Debomita, B., Nagothy, P., Mamindla, P.R., Arindam, T., 2019. Ligand-Based Pharmacophore Modeling, Virtual Screening and Molecular Docking Studies for Discovery of Potential Topoisomerase I Inhibitors. *COMPUT STRUCT BIOTECH* 17, 291–310.
- Sudharsan, S., Orr, H.S., Carmit, Z., Omer, B., Varda, Z., Edward, S., 2019. Synergistic Inhibition of Mycotoxigenic Fungi and Mycotoxin Production by Combination of Pomegranate Peel Extract and Azole Fungicide. *front microbiol.* 10, 1919.
- Thommas, M., Özlem, T.B., 2019. South African Abietane Diterpenoids and Their Analogs as Potential Antimalarials: Novel Insights from Hybrid Computational Approaches. *Molecules* 24, 4036.
- Usha, P.S., Preetida, J.B., Anupam, V., 2017. Aflatoxins: Implications on Health. *IJCB* 32 (124), 133.
- Williams, J.H., Phillips, T.D., Jolly, P.E., Stiles, J.K., Jolly, C.M., Aggarwal, D., 2004. Human Aflatoxicosis in Developing Countries: A Review of Toxicology, Exposure, Potential Health Consequences, and Interventions. *Am J Clin Nutr.* 80, 1106–1122.